Hindawi
Shock and Vibration
Volume 2024, Article ID 5527946, 18 pages
https://doi.org/10.1155/2024/5527946

Research Article

Efficacy of the Combined Use of Bed Sill and Sacrificial Piles to Control Local Scour around Circular Bridge Piers

Vahid Javidi Vahdati,[1] Ahmad Ahmadi,[1] Amirabbas Abedini,[1] and Manouchehr Heidarpour[2]

[1]*Department of Water and Hydraulic Structures Engineering, College of Civil Engineering, Shahrood University of Technology, Shahrood 3619995161, Iran*
[2]*Department of Water Science and Engineering, College of Agriculture, Isfahan University of Technology, Isfahan 8415683111, Iran*

Correspondence should be addressed to Manouchehr Heidarpour; heidar@iut.ac.ir

Received 1 December 2023; Revised 18 February 2024; Accepted 13 March 2024; Published 26 March 2024

Academic Editor: Xiuquan Liu

In this study, the results are presented and discussed from laboratory test campaigns specifically designed to investigate the behavior of sacrificial piles as a countermeasure against local scouring at a circular bridge pier and clear-water conditions with flow intensity slightly below the threshold of sediment motion. Sacrificial piles are assessed on the upstream side of the pier in two transverse and triangular arrangements. Piles can reduce scouring by deflecting the flow and creating a low-velocity wake region behind them. The efficiency of the piles against local scouring depends on the diameter of the piles, the number of piles, and the angle of the wedge. The investigation was aimed at evaluating the effectiveness of the sacrificial piles as a function of different dimensionless groups. It was found that the triangular arrangement of sacrificial piles has better results than the transverse arrangement. The results showed that the triangular sacrificial piles reduced the maximum local scour depth at the pier to 37.2% in the best configuration. Combined countermeasures were tested, which were composed of sacrificial piles and a bed sill downstream of the pier; in the best configuration, the scour depth reduction in front of the pier reached 51.1%. The increased efficiency of the combination of bed sill and sacrificial piles (BSSP) is an advantage that can reduce the risk of pier failure when the duration of the flood is short. This last result shows that a combination of BSSP may be a very effective countermeasure against local scouring at bridge piers. Finally, the coherent turbulent flow structure around the best combination of BSSP was investigated, and its effect on the bed scouring pattern was studied. A 3D analysis of the bursting process was used. Turbulence characteristics, as well as the occurrence and transition probabilities of bursting events, were calculated. The obtained results confirmed the quite effective effect of the combination of these two countermeasures in reducing the scour depth.

1. Introduction

Estimation of scour around a pier is one of the most important and challenging issues in hydraulic engineering. The bridge pier, as a barrier against the stream flow, causes the flow separation. Due to this separation, the stream flow, as a result of passing over the sides of bridge piers, causes local scouring around the pier [1]. Local scouring has been reported as the main cause of the failure and instability of many bridges [2–5]. Therefore, investigation of the scour phenomenon and the ways to control it seems to be necessary for the safer design of bridges. The main mechanisms of local scour include downflow, horseshoe vortex, and wake vortices. To control the negative effects of these factors on local scouring, two methods of bed armoring countermeasures and flow-altering methods have been proposed in the literature [6–9]. In this study, two countermeasures (bed sill and sacrificial piles) of the flow-altering methods were combined and evaluated.

1.1. Combinations of Scouring Countermeasures in Previous Literature. The bed sill is placed as a barrier against sediment transport downstream of the pier to prevent the scour development and reduce the erosive force of wake vortices. Sacrificial piles are piles serving as a protection factor in the upstream of the pier; they themselves are exposed to scour to protect the bridge pier against local scour. In the past, these countermeasures have been used individually, for example, Grimaldi et al. [10] and Tafarojnoruz et al. [8] for bed sill and Melville and Hadfield [6] and Haque et al. [11] for sacrificial piles.

The combined countermeasures have been investigated in the previous studies [12, 13]. However, among the combinations of countermeasures that have been implemented, the inappropriate combination of two countermeasures, rather than each countermeasure, may not have a significant effect on reducing scour depth. Table 1 presents a summary of the results of some past studies in relation to the combination of countermeasures. In this table, the term r_{de} (%) is defined as the percentage reduction of the pier scour depth. Three modes could be distinguished for the combination of two countermeasures, as compared to each alone. The combination of two countermeasures may not be effective at all, be less effective, or be quite effective. A combination is quite effective when the efficiency of the combined countermeasures is almost close to the sum of the efficiency of each individual countermeasure and/or even greater than their sum. For example, the combination of sacrificial piles and collar [13] is not effective at all; meanwhile, the combination of slot and bed sill [10] is less effective, and that of cable and collar [7] can be quite effective (according to Table 1). The conducted investigations show that the combination of countermeasures is of great importance in reducing scour depth. According to Table 1, most of the combined countermeasures are quite effective, but the combination of some countermeasures is not efficient. Therefore, one should be very careful when choosing them.. To the authors' knowledge, a combination of BSSP has not been studied for reducing local scour at bridge piers. In this paper, we present the results of an experimental study.

Investigations showed that the combination of sacrificial piles with countermeasures such as collars, pier slots, and cable was not effective in reducing the local scour (Table 1). The literature results are not strictly comparable, for example, in order to establish if sacrificial piles have a greater efficiency when combined with other countermeasures. The efficiency of sacrificial piles can decrease in oblique flow [6, 26, 27]. Experiments conducted by Melville and Hadfield [6] and Chiew and Lim [26] revealed that sacrificial piles lose their effectiveness to a large extent under high flow velocities, i.e., for $U > U_c$. Piles cannot be reliable during typical flood conditions [28]. There is no guarantee that there will be a complete elimination of local scour. Therefore, further research is needed to confirm the potential effectiveness of this countermeasure. The principal objective of this study was to evaluate the effectiveness of sacrificial piles as a function of $(N_P D_P/D)$ and (α), where, $N_P D_P/D$ = blockage ratio of sacrificial piles and α = angle of the wedge and of the combined countermeasures, composed of sacrificial piles and a bed sill downstream of the pier (Figure 1).

1.2. Turbulent Flow Structure. The results of the previous studies have shown that research has mainly focused on determining the scour depth and how it can be controlled. In addition, although there have been studies on the evaluation of the complex flow structure around the pier, more research is needed. Some researchers have tried to understand the complex flow structure, but this field still needs more research [25, 29, 30]. Keshavarzi et al. [31] used the 3D analysis of the bursting process (octant analysis) to investigate the flow structure around the bridge pier. It should be noted that 2D and 3D bursting processes have been used on ripples as well as in meandering channels [32–34].

Multiple studies were performed in an open channel using 2D quadrant analysis. However, the flow around the piers is fully 3D [31]. Therefore, the technique used in this study (octant analysis) provides more resolution to the effect of transverse velocity fluctuations in the sediment particle entrainment process. Although Keshavarzi et al. [31] investigated the characteristics of turbulent flow around a single bridge pier using three-dimensional analysis of bursting processes, to the writers' knowledge, in the literature, the coherent turbulent flow structure in the pier combination with BSSP has not been investigated. The objective of this study is to provide a better understanding of the 3D flow around this model, the interactions between its elements, and their effects on this flow field. Here, after determining the efficiency of the best type of combination of BSSP, experiments were conducted with the aim of obtaining the contribution of eight different bursting events.

2. Materials and Methods

2.1. Dimensional Analysis. The dimensional analysis presented in this section is used to discuss the effect of dimensionless groups on local scour depth. For a smooth circular pier with countermeasures, the relation between the local scour depth at the bridge pier d_s and its dependent parameters can be expressed as follows:

Table 1: A summary of the results of the combined countermeasures.

Researchers	Combined countermeasures	r_{de} (%)
Gaudio et al. [13]	Submerged vanes	12.4
	Bed sill	17.2
	Sacrificial piles	32.2
	Collar	28.7
	Slot	33.2
	Submerged vanes and bed sill	25.3
	Sacrificial piles and collar	36.2
	Sacrificial piles and slot	38.1
	Slot and collar	81.8
	Bed sill and collar	46.2
Chiew [14]	Slot	20
	Collar	20
	Slot and collar	100
Grimaldi et al. [10]	Slot	30
	Bed sill	26
	Slot and bed sill	45
Soltani-Gerdefaramarzi et al. [15]	Jet injection	30
	Bed suction	9
	Jet injection and bed suction	50.4
Moncada-M et al. [16]	Collar	55 to 96
	Slot	60 to 88
	Collar and slot	100
Mashahir et al. [17]	Collar	23
	Collar and bars	27
Shahkarami [18]	Bed sill	20
	Collar	65
	Bed sill and collar	75
Mazloom et al. [19]	Slot	25
	Submerged vanes	35
	Slot and submerged vanes	86
Zomorodian et al. [20]	Sacrificial piles	46.67
	Collar	70
	Slot	31
	Sacrificial piles and collar	75
	Sacrificial piles and slot	63
	Slot and collar	73
Aghli and Zomorodian [21]	Cable	59
	Collar	55
	Cable and collar	69.7
Shojaei et al. [22]	Submerged vanes	2
	Collar	35
	Submerged vanes and collar	61
Izadinia and Heidarpour [7]	Cable	12.85
	Collar	28.57
	Cable and collar	52.85
Tafarojnoruz et al. [23]	Collar	28.7
	Collar and bed sill	64.5
Javidi-Vahdati et al. [24]	Sacrificial piles	55
	Sacrificial piles and cable	60
Gerami et al. [25]	Bed sill	25.4
	Cable	13.4
	Bed sill and cable	34.4

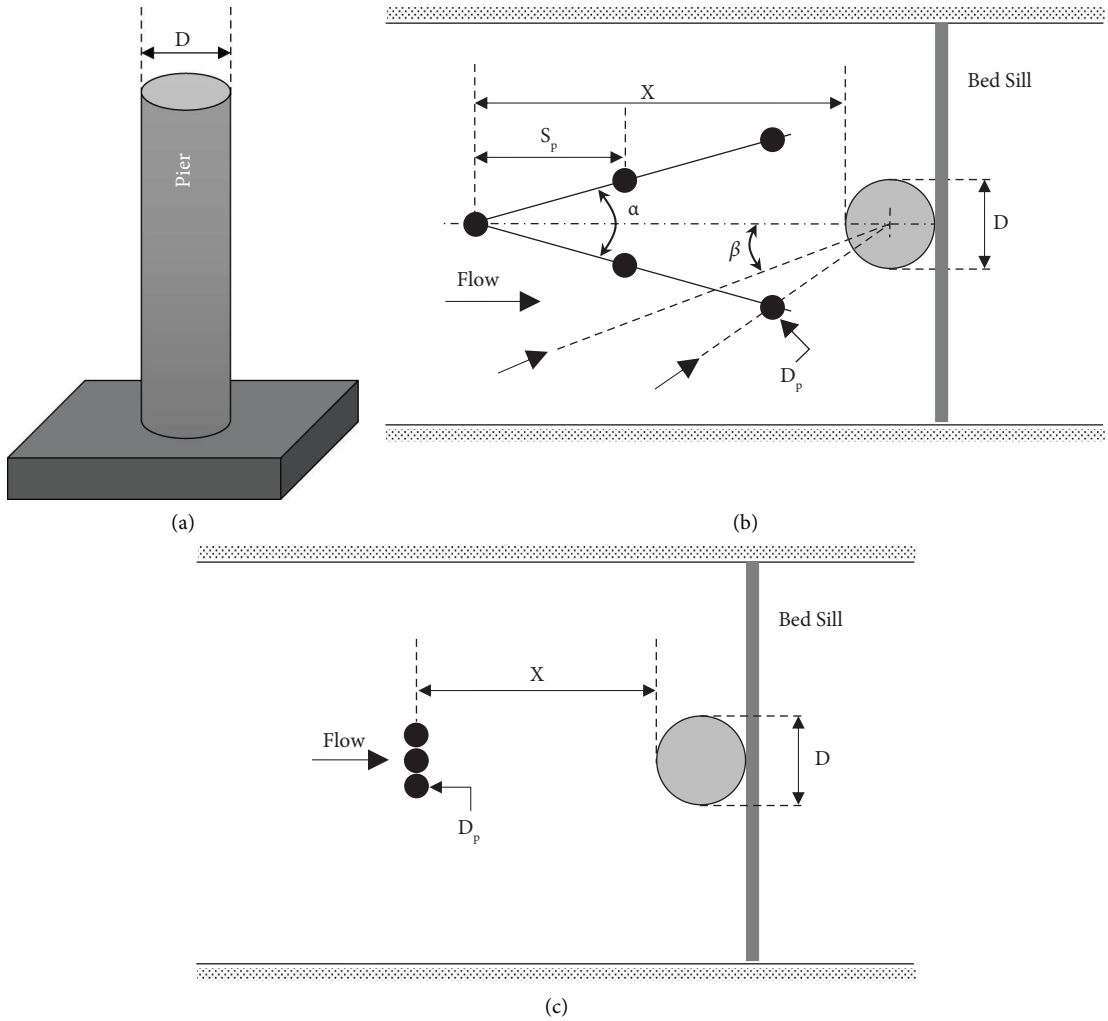

Figure 1: (a) Circular cylindrical pier, (b) bed sill and triangular sacrificial piles, and (c) bed sill and transverse sacrificial piles.

$$d_s = f\left\{\begin{array}{c} \text{flood flow } (g, \rho, \nu, U, y), \\ \text{bed sediment } \left(\rho_s', d_{50}, \sigma_g, U_c\right), \\ \text{bridge pier geometry } (D), \\ \text{flume geometry } (B), \\ \text{time } (t), \\ \text{bed sill characteristics } (L_{bs}), \\ \text{sacrificial pile characteristics } \left(D_p, S_p, X, N_p, \alpha, \beta\right), \end{array}\right\}, \tag{1}$$

where f = unknown function, g = acceleration of gravity, ρ = water density, ν = kinematic viscosity of water, U = mean approach flow velocity, y = flow depth, ρ_s' = submerged sediments density, d_{50} = mean sediment particle size, σ_g = geometric standard deviation, U_c = critical flow velocity, D = circular pier diameter, B = channel width, t = time, L_{bs} = distance between the bed sill and pier, D_p = sacrificial piles diameter, S_p = distance between the piles, X = displacement distance, N_p = number of piles, α = angle of the wedge, and β = deviation angle between the approach flow and pier axis (skew angle). When the Buckingham theorem is applied to equation (1), with ρ, U, and D as basic variables, the following dimensionless relations are obtained:

$$\frac{d_s}{D} = f\left(\frac{U}{\sqrt{gD}}, \frac{y}{D}, \frac{\rho_s'}{\rho}, \frac{D}{d_{50}}, \sigma_g, \frac{U}{U_c}, \frac{B}{D}, \frac{Ut}{D}, \frac{L_{bs}}{D}, \frac{D_p}{D}, \frac{S_p}{D}, \frac{X}{D}, \frac{N_p D_p}{D}, \alpha, \beta\right), \tag{2}$$

where $F_P = U/\sqrt{gD}$ = pier Froude number, y/D = flow shallowness, ρ_s'/ρ = submerged sediment specific gravity, D/d_{50} = sediment coarseness, σ_g = sediment nonuniformity, U/U_c = flow intensity, B/D = sidewall effects, Ut/D = time scale for the scour development, $N_P D_P/D$ = blockage ratio of sacrificial piles, α = angle of the wedge, and β = deviation angle between the approach flow and pier axis (skew angle).

The following considerations can be applied to determine the effect of dimensionless groups in equation (2): (1) if $y/D \geq 2.5$, shallowness effects are insignificant and can be ignored [26, 35], (2) for sand and gravel, $\Delta = \rho_s'/\rho$ is almost constant and equal to ≈1.65, (3) for uniform sediment with $\sigma_g < 1.5$ and $25 \leq D/d_{50} \leq 130$ can be maximized as d_s [27], (4) if $U/U_c \approx 1$, the maximum scour depth is obtained under clear-water flow conditions, (5) if $B/D \geq 10$, the channel sidewall (or blockage) effects on the local scour, which is due to the pier presence, are ignored [26, 36], (6) for the bed sill attached to the back of the pier, L_{bs}/D is practically ineffective, (7) in the pile arrangement, D_P, S_P and X are assumed to be constant and there is no β, and (8) in this study, the constant flow conditions were considered, so Fr is constant. According to the abovementioned considerations for the present study, the dimensionless local scour depth in equation (2) becomes simple which is described as follows:

$$\frac{d_s}{D} = f\left(\frac{Ut}{D}, \frac{N_p D_p}{D}, \alpha\right). \tag{3}$$

At equilibrium, the variation of d_s/D against time is almost negligible, so Ut/D is practically ineffective. To maximize the efficiency of the two countermeasure combinations, such as bed sill and sacrificial piles, particular values should be considered for the dimensionless groups, which will be explained in the subsequent sections.

2.2. Experimental Setup and Procedure. The experiments of this study were carried out in a glass flume with a recirculating flow system in the hydraulic laboratory of the Isfahan University of Technology. The floor and side walls of this flume were made of glass. This helped us to have a better side view of the flow and sediment movement in the flume. The flume consisted of a rectangular cross-section with a floor width of 0.9 m, a height of 0.6 m, and a length of 15 m.

It should be noted that an electromagnetic flow meter and a point gauge were used to measure the discharge and the flow depth, respectively. A tailgate at the downstream end of the flume was also used to control the flow depth. The length of the test section was 3 m, which consisted of 3 sections 0.18 m deep. A recess (middle section) of one meter length was embedded between two upstream and downstream Teflon plates (where the pier was located). The upstream Teflon plates were installed at 0.16 m above the flume bottom and covered with sediments up to 0.02 m. The downstream Teflon plate was considered to be flush with the bed (deep = 0.18 m) for the full development of the bed morphology. The pier was mounted vertically on the flume bottom at a distance of 10 m from the flume inlet, where the flow was fully developed. The fully developed flow region was determined by measuring the velocity profiles along the flow from the flume inlet when no bed was installed in the channel. The fully developed flow region is where there was no detectable change in velocity profiles in the flow direction. The recess was filled with the uniform sediment (d_{50} = 0.77 mm and σ_g = 1.06). A thin layer of uniform sand of the same size was glued over the false floor to roughen it. A 6 cm-diameter circular PVC was used as the pier model. According to Chiew and Melville [26], the pier diameter should not be more than 10% of the width of the channel to prevent the effect of the channel sidewalls on scour. The pier was embedded at the centerline of the channel. All experiments were conducted in clear-water conditions, because the maximum scour depth in these conditions occurred at the threshold of the bed material motion [37]. The value of U was determined by preliminary tests before the pier was installed. The experiments were carried out under flow conditions with constant flow depth and flow intensity. The flow conditions in the experimental tests and dimensionless groups were considered according to Table 2. These could satisfy the conditions presented in the Dimensional Analysis section. U_{*c} was calculated from the Shields diagram. Scour depth in front of the pier was measured by a meter attached to the pier body. Contraction scour was not observed in any experiment, since the scour holes were completely developed in the transverse direction.

In this study, the countermeasure of sacrificial piles was used to reduce scour, and finally, it was combined with the bed sill. Triangular and transverse arrangements of sacrificial piles were used. Table 3 shows the geometric parameters of sacrificial piles. A 1 cm-thick PVC as wide as the channel, flush with the bed and extended to the floor of the channel, was used as the bed sill. According to Grimaldi et al. [10] and Tafarojnoruz et al. [8], the best configuration of the bed sill is when it is attached to the back of the pier. In this study, the bed sill was attached to the downstream end of the pier according to the suggested best configuration. The circular pier model, the arrangement of sacrificial piles with geometric parameters, and the combination of BSSP are shown in Figure 1.

Fourteen experiments were performed. The scour depth was measured in both unprotected and protected piers for comparison. A summary of the experiments and various combinations of the sacrificial piles' group and bed sill with their geometric parameters and efficiency are given in Table 4. The first column shows the name of the test. Test C1, which was for the pier without countermeasures, was used as the reference to evaluate the effectiveness of the countermeasures. The experiments were designed based on neglecting the effect of side walls, sediment particle size, flow

Table 2: Experimental conditions and dimensionless groups.

D (cm)	d_{50} (mm)	Q (m^3/s)	y (cm)	U (m/s)	U_c (m/s)	U_{*c} (m/s)	U/U_c	D/d_{50}	B/D	B/y	y/D	Fr
6	0.77	0.05	19	0.292	0.326	0.0181	0.9	77.9	15	4.7	3.2	0.21

Table 3: Geometric parameters of sacrificial piles.

Pile arrangement	N_p	X/D	D_p	S_p	α	β
Triangular	3, 5	2.5	$D/6$	D	30°, 60°	—
Transverse	3, 5	2	$D/6$	—	—	—

viscosity, and flow shallowness, as described in the previous section. The percent efficiency of BSSP at the end of each test, r_{de} can be calculated by the following equation:

$$r_{de} = \frac{d_{se0} - d_{se}}{d_{se0}} \times 100\,(\%), \tag{4}$$

where d_{se0} and d_{se} are the equilibrium scour depths in front of the unprotected and protected piers, respectively. Also, d_{se0} and d_{se} were measured at the end of each experiment.

According to the literature, there are various criteria to identify the equilibrium conditions [38–43]. However, in general, it takes several days to achieve an acceptable equilibrium scour depth. Therefore, in this study, all experiments were not continued until reaching the equilibrium state. The duration of stopping the experiments was determined as follows.

First, a relatively long experiment (36 hours) was performed (Figure 2). Then, using the following two standard criteria, the duration of stopping the experiments was obtained: (1) slope change in the semilogarithmic plot by plotting d_s versus log t [39] and (2) it was found that 90% of the final scour depth occurred during the first eight hours, which was consistent with the findings of [44]. Therefore, in this study, all experiments continued for 8 hours.

2.3. Flow Structure. In this study, a 3D downward-facing ADV (accuracy ± 0.1 m/s) was used to measure the 3D velocity components at the pier centerline at a distance of 2 mm from the bed surface (Figure 3). The ADV probe was placed 5.5 cm above the bed, and the velocities were measured in the sampling volume with a height of 5 mm and a diameter of 6 mm. The velocity components in the centerline from upstream to downstream were taken first for the unprotected pier (test C1) and then for the best combination of BSSP (Figure 4). The sampling frequency was set at 200 Hz [45]. Moreover, the sampling durations were assumed to be 120 s in order to have a statistically independent time-averaged velocity, as done by Ge et al. [46]. Velocity components were measured at each point with these settings. Measurements were made by a bed fixed at the end of the experiment. Investigation of the flow structure was performed by removing the weakly measured data. For this purpose, the data were filtered by the WinADV software. Two parameters, including signal-to-noise ratio (SNR) and correlation coefficient (COR), were constantly controlled during the experiment to collect good data. In the best ranges, to provide good data, SNR and COR should be greater than 15 dB and 70%, respectively [31, 47, 48]. These values were applied to filter the data in the WinADV software. In addition, the filter provided by Goring and Nikora [45] has been used for phase-space threshold despiking to detect and eliminate the spurious data.

2.3.1. Turbulence Characteristics. Velocity components were measured in three directions: streamwise or x-axis (u-velocity), transverse or y-axis (w-velocity), and vertical or z-axis (v-velocity). Turbulence characteristics could be determined and investigated by velocity fluctuations. The following relations are defined for the velocity fluctuations u', w', and v':

$$\begin{aligned} u' &= u_i - \bar{u}, \\ w' &= w_i - \bar{w}, \\ v' &= v_i - \bar{v}. \end{aligned} \tag{5}$$

The temporal-averaged velocities are determined by using the following relationships:

$$\begin{aligned} \bar{u} &= \frac{1}{N}\sum_{i=1}^{N} u_i, \\ \bar{w} &= \frac{1}{N}\sum_{i=1}^{N} w_{i,}, \\ \bar{v} &= \frac{1}{N}\sum_{i=1}^{N} v_i. \end{aligned} \tag{6}$$

Turbulence characteristics have multiple parameters. Here, turbulent kinetic energy and Reynolds' shear stress will be reviewed. The total turbulent kinetic energy of the flow (TKE_{xyz}) is defined according to the following equation. TKE relationships in different directions are also given here:

Table 4: Details of various combinations from the group of bed sill and sacrificial piles with geometric parameters and efficiency.

Test	Combined countermeasures	Geometric parameters of sacrificial piles					d_{se0}, d_{se} (cm)	r_{de} (%)
		Arrangement of piles	N_p	N_pD_p/D	X/D	α		
C1	—	—	—	—	—	—	9	—
C2	Bed sill	—	—	—	—	—	7.4	17.8
C3	Sacrificial piles	Transverse	3	0.5	2	—	6.8	24.4
C4	Sacrificial piles	Transverse	5	0.83	2	—	7.55	16.1
C5	Bed sill and sacrificial piles	Transverse	3	0.5	2	—	5.4	40
C6	Bed sill and sacrificial piles	Transverse	5	0.83	2	—	6.15	31.7
C7	Sacrificial piles	Triangular	3	0.5	2.5	30°	5.65	37.2
C8	Sacrificial piles	Triangular	5	0.83	2.5	30°	5.8	35.6
C9	Bed sill and sacrificial piles	Triangular	3	0.5	2.5	30°	4.4	51.1
C10	Bed sill and sacrificial piles	Triangular	5	0.83	2.5	30°	4.7	47.8
C11	Sacrificial piles	Triangular	3	0.5	2.5	60°	7	22.2
C12	Sacrificial piles	Triangular	5	0.83	2.5	60°	7.5	16.7
C13	Bed sill and sacrificial piles	Triangular	3	0.5	2.5	60°	5.7	36.7
C14	Bed sill and sacrificial piles	Triangular	5	0.83	2.5	60°	6.35	29.4

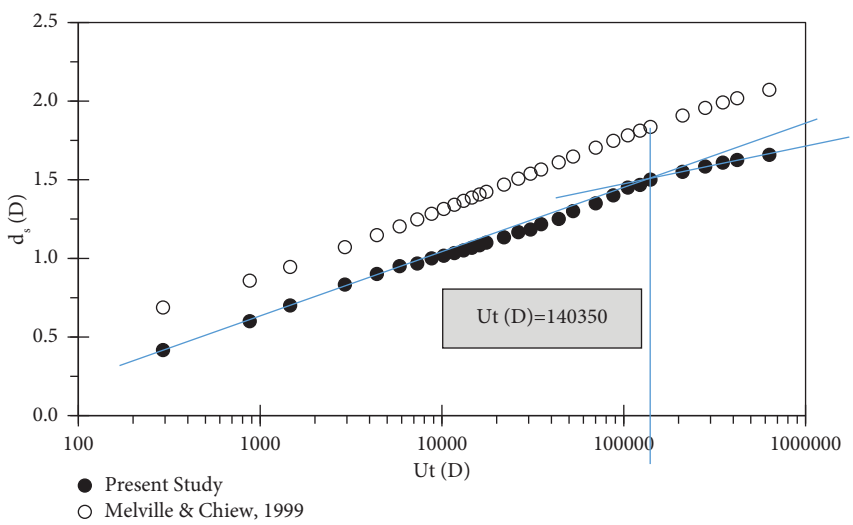

Figure 2: Time development of scour to determine the equilibrium time.

Figure 3: Acoustic Doppler velocimetry (ADV) in the laboratory.

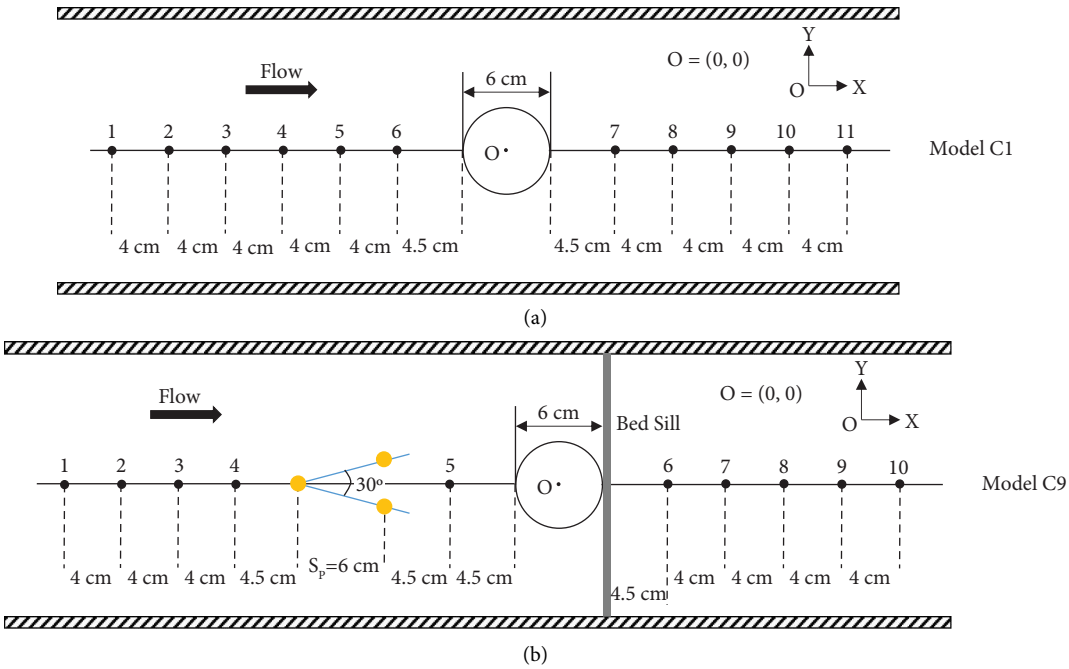

Figure 4: Measuring positions of velocity components from upstream to downstream of the centerline: (a) test C1 and (b) test C9.

$$TKE_{xyz} = \frac{1}{2}\left(\overline{u'^2} + \overline{w'^2} + \overline{v'^2}\right),$$
$$TKE_x = \frac{1}{2}\left(\overline{u'^2}\right),$$
$$TKE_y = \frac{1}{2}\left(\overline{w'^2}\right), \quad (7)$$
$$TKE_z = \frac{1}{2}\left(\overline{v'^2}\right).$$

Reynolds' shear stress in the xz and yz planes is calculated as follows:

$$\tau_{xz} = -\rho\overline{u'v'},$$
$$\tau_{yz} = -\rho\overline{w'v'}. \quad (8)$$

2.3.2. 3D Analysis of Bursting Events. 3D bursting events include eight types of events, which are classified into class A (internal) and class B (external). The classification of these events is performed based on the sign of the velocity fluctuations, as presented in Table 5.

Based on octant analysis, 3D bursting events exist in 8 octant zones. P_k is calculated based on n_k, and "k (subscript) represents each octant zone ($k = 1$–8)":

$$P_k = \frac{n_k}{N},$$
$$N_t = \sum_{k=1}^{8} n_k. \quad (9)$$

Occurrence probabilities alone are unable to determine and diagnose the state of sediment entrainment, so it is necessary to determine the transition probabilities. Based on eight events of the 3D bursting process, 64 probable movements can be considered. A change in the situation from one zone to the same zone or another zone in a time series is defined as movement. The movement of events is determined based on the Markov process. According to the Markov process, the transition probabilities of events from zone i to zone j in a time series from t to $t+1$ are determined by using the following relationship:

$$P_{i\longrightarrow j} = \frac{n_{i\longrightarrow j}}{n_i} \quad i, j = 1 - 8, \quad (10)$$

where

$$n_i = n_{i\longrightarrow 1} + n_{i\longrightarrow 2} + \cdots + n_{i\longrightarrow 8}. \quad (11)$$

Considering the abovementioned definition, 64 probable movements can be recognized for each point. Figure 5 shows the matrix view of 64 probable movements.

3. Results and Discussion

3.1. Validation of Local Scour Depth Results. A review of the related literature shows that to improve the design of bridges, efforts have been made to understand the scour phenomenon and temporal variation of scour depth around the bridge piers [5, 7, 41, 49]. Some researchers have also proposed relationships to estimate the scour depth at different times [41, 50, 51]. As can be seen in Figure 6, the comparison of the temporal variations of the experimental values of d_s/D and the values calculated from these equations can be seen. A good agreement between the results of the present study and those of Barkdoll [50] and Guo [51] was observed at the equilibrium time. The findings showed that a high percentage of scour depth occurred in the early

Table 5: Classification of three-dimensional bursting events.

Events	u'	w'	v'
Internal outward interaction (I-A)	+	+	+
Internal ejection (II-A)	−	−	+
Internal inward interaction (III-A)	−	−	−
Internal sweep (IV-A)	+	+	−
External outward interaction (I-B)	+	−	+
External ejection (II-B)	−	+	+
External inward interaction (III-B)	−	+	−
External sweep (IV-B)	+	−	−

$$P(I) = \begin{vmatrix} P_{1\Rightarrow1} & P_{1\Rightarrow2} & P_{1\Rightarrow3} & P_{1\Rightarrow4} & P_{1\Rightarrow5} & P_{1\Rightarrow6} & P_{1\Rightarrow7} & P_{1\Rightarrow8} \\ P_{2\Rightarrow1} & P_{2\Rightarrow2} & P_{2\Rightarrow3} & P_{2\Rightarrow4} & P_{2\Rightarrow5} & P_{2\Rightarrow6} & P_{2\Rightarrow7} & P_{2\Rightarrow8} \\ P_{3\Rightarrow1} & P_{3\Rightarrow2} & P_{3\Rightarrow3} & P_{3\Rightarrow4} & P_{3\Rightarrow5} & P_{3\Rightarrow6} & P_{3\Rightarrow7} & P_{3\Rightarrow8} \\ P_{4\Rightarrow1} & P_{4\Rightarrow2} & P_{4\Rightarrow3} & P_{4\Rightarrow4} & P_{4\Rightarrow5} & P_{4\Rightarrow6} & P_{4\Rightarrow7} & P_{4\Rightarrow8} \\ P_{5\Rightarrow1} & P_{5\Rightarrow2} & P_{5\Rightarrow3} & P_{5\Rightarrow4} & P_{5\Rightarrow5} & P_{5\Rightarrow6} & P_{5\Rightarrow7} & P_{5\Rightarrow8} \\ P_{6\Rightarrow1} & P_{6\Rightarrow2} & P_{6\Rightarrow3} & P_{6\Rightarrow4} & P_{6\Rightarrow5} & P_{6\Rightarrow6} & P_{6\Rightarrow7} & P_{6\Rightarrow8} \\ P_{7\Rightarrow1} & P_{7\Rightarrow2} & P_{7\Rightarrow3} & P_{7\Rightarrow4} & P_{7\Rightarrow5} & P_{7\Rightarrow6} & P_{7\Rightarrow7} & P_{7\Rightarrow8} \\ P_{8\Rightarrow1} & P_{8\Rightarrow2} & P_{8\Rightarrow3} & P_{8\Rightarrow4} & P_{8\Rightarrow5} & P_{8\Rightarrow6} & P_{8\Rightarrow7} & P_{8\Rightarrow8} \end{vmatrix}$$

Figure 5: Transition probabilities' matrix of events.

hours. According to Ettema [35], the scour process consists of three separate phases, including the initial phase, the principal phase, and the equilibrium phase. In the initial phase, the most intense state of scour formation occurs. The difference in the results could be attributed to the differences in different experimental conditions, including flow intensity (U/U_c).

3.2. Performance of the BSSP. As can be seen in Table 4, the test results at the same flow conditions for all tests are expressed in terms of percentage scour depth reduction and compared to the pier without countermeasures. In clear-water conditions, the scoured sediments around the sacrificial piles are partially deposited around the pier, leading to a reduction in the scour depth around the pier and consequently, increasing the efficiency [8, 11]. In the combination of two countermeasures, the performance is better when the protection mechanism of one device also supports the other device [9]. According to Table 4, the simultaneous combination of BSSP had good efficiency in reducing the local scour depth and could be quite effective. The efficiency of this combination was approximately equal to the sum of the efficiency of each individual countermeasure.

The good efficiency in the results obtained from the combination of these two countermeasures could be attributed to the good interaction between these two countermeasures. The strength of the wake vortices at downstream of the pier is reduced by the bed sill. On the other hand, the wake vortices created behind the piles have low erosive power and transfer fewer sediments to the back of the pier. Thus, these two wake vortices together have led to a far greater scour depth reduction than any individual countermeasure. The results of Table 4 show that the combination of BSSP can be considered as an efficient combination to reduce the local scour.

Field applications of countermeasures have several problems, which can limit their practical use. Among these problems, we can point out the accumulation of floating debris around the sacrificial piles, which affects the performance of the piles. Rivers carry appreciable quantities of floating debris during floods. Such material accumulates in the form of large masses around the sacrificial piles, sometimes referred to as debris rafts. Additional flow obstruction causes scour depths in excess of the scouring depth of the pier without pile [28, 52]. Therefore, debris accumulation reduces the efficiency of sacrificial piles. In the literature, there are several studies that have investigated the effect of debris accumulation [53–55]. It should be noted that in this study, the effect of debris accumulation on the efficiency of sacrificial piles was not studied.

The effectiveness of sacrificial piles is dependent on the number of piles, the diameter of piles, partial or full submergence, flow intensity (U/U_c), geometric arrangement in relation to each other, and bridge pier [6, 9, 28]. The results show that with the increase in pile numbers, the performance decreased for both individual sacrificial piles and their combination with bed sill. Melville and Hadfield [6] showed that by increasing the number of piles in the same arrangement, the performance increased from 48% to 56%.

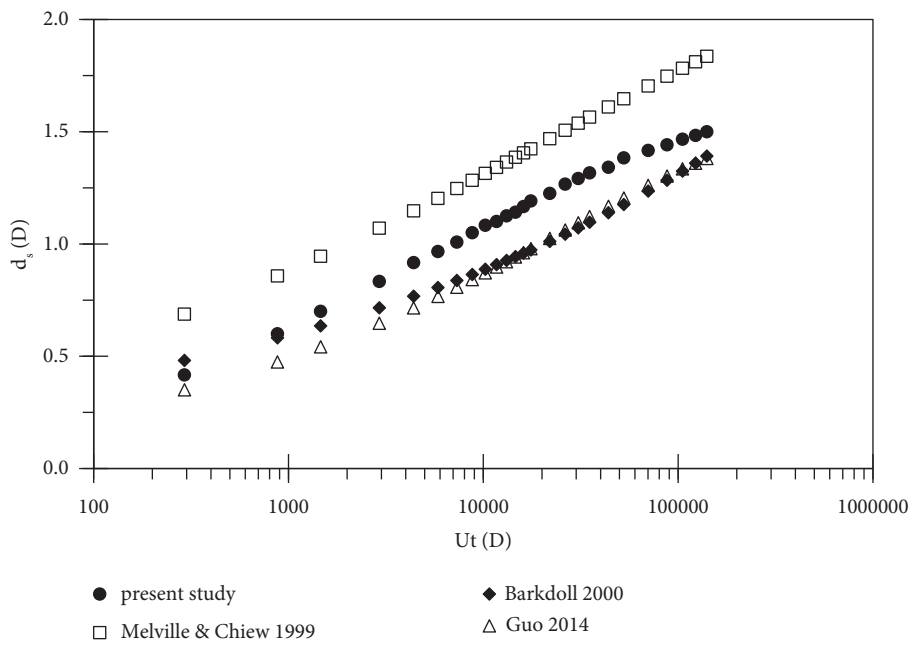

Figure 6: Temporal variations of the local scour around unprotected pier (C1) and comparison with other studies.

Meanwhile, Tafarojnoruz et al. [8] found that the performance was decreased from 32.2% to 5.5% with increasing the number of piles in the same arrangement. By increasing the pile number, the wake region produced by the sacrificial piles was enlarged, and local scour reduction was expected to be improved [9]. However, the piles should be placed such that the piles that are rear can be on the edge of the wake region of an upstream pile [6]. In this case, the width of the wake of the entire group is increased, and as a result, the local scour reduction is improved; otherwise, we will witness the opposite result. This is because when the rear piles are not placed on the edge of the wake region of an upstream pile, the high-velocity flow enters the regions between the piles, affecting the pier. Thus, the performance decreased.

The results, as represented in Table 4, showed that increasing the wedge angle decreased the efficiency. In an arrangement with the same number and the same spacing between piles and bridge pier, when the wedge angle was increased, the transverse edge-to-edge distance of the rear piles with the upstream piles was raised too. As a result, the flow could easily pass between the piles and affect the pier, thus reducing the performance of the piles. Melville and Hadfield [6] also reported a decrease in the performance of piles with an increase in the wedge angle.

In past studies, the triangular arrangement of sacrificial piles with the apex of the triangle pointing upstream has been considered one of the best configurations among the other tested cases [6]. According to Table 4, the highest and best efficiency in the combination of BSSP was related to test C9, whose efficiency was as much as 51.1% in front of the pier. Therefore, in the following sections, we focus on the flow structure around this combination (test C9). For comparison, the results of the pier without countermeasures (test C1) are included. Figure 7 shows the pictures related to the tests performed for C1 and C9. As in test C9, it can be seen that while the bed sill protects the pier, excess scouring occurs downstream (Figure 7(B3)). A similar problem was found when using the bed sill downstream of hydraulic structures [56, 57].

3.3. Turbulent Kinetic Energy. In this section, as in other subsequent sections, an investigation of the flow structure along the channel centerline (the pier centerline) from upstream to downstream has been carried out around the two models C1 and C9. Variations of TKE_{xyz} along the centerline are shown in Figure 8. For comparison, the longitudinal variations of TKE_x, TKE_y, and TKE_z are included. Right in the two positions in front and behind the unprotected pier, the *TKE* values in the transverse direction are higher than those in the longitudinal and vertical directions. Meanwhile, in the same position at the protected pier (the position between the pier and sacrificial piles), the *TKE* values in the longitudinal direction are higher than those in other directions. Therefore, using the simultaneous combination of BSSP decreases the transverse effect of velocity on the sediment particle entrainment; it also reduces the local scour depth in front of the pier. It also impedes the development of a scour hole in front of the pier. A significant decrease in TKE_{xyz} and TKE_x values was observed in the downstream of the protected pier with BSSP compared to the unprotected pier. Similar results were also observed by Gerami et al. [25] and Nezhadian and Hamidifar [58]. The transverse component of the velocity has a significant value, i.e., in the downstream of the pier, a high shear layer is created and the flow is very turbulent [31]. The high TKE_{xyz} in the downstream of the pier is directly related to the erosive sediment particles, which could be visible in the case of the unprotected pier in Figure 7(a).

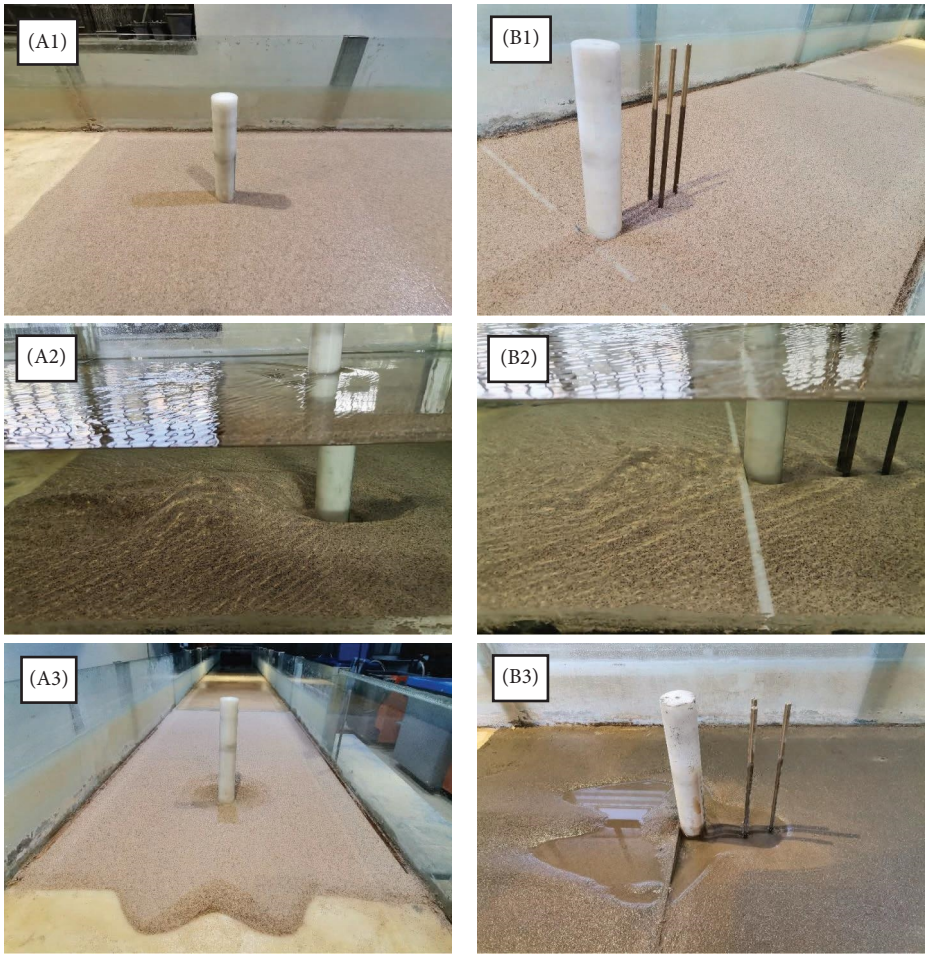

(a) (b)

Figure 7: Pictures of the scour experiments at the inception of the test (no. 1), during the test (no. 2), and at the end of the test (no. 3) for (a) test C1 and (b) test C9.

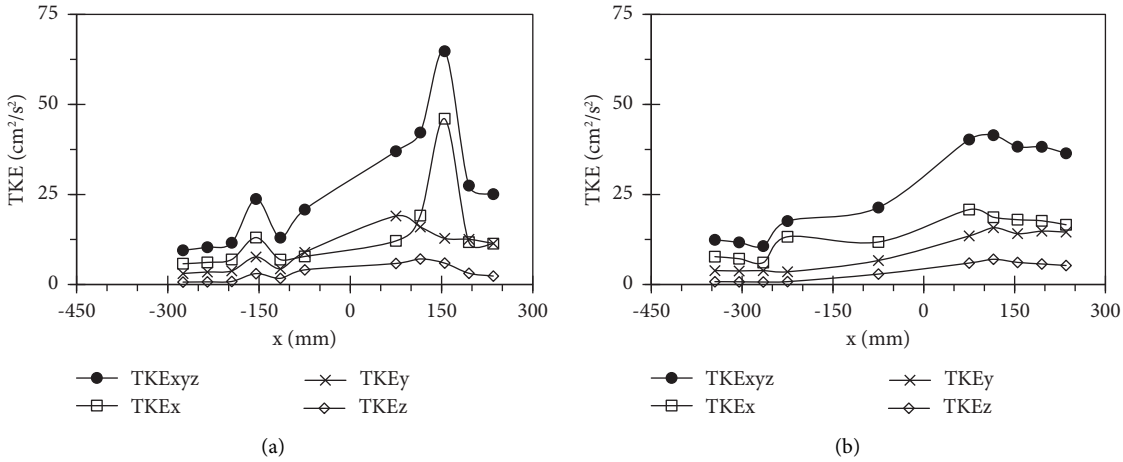

Figure 8: Longitudinal variation of turbulent kinetic energy in the channel centerline for (a) unprotected pier (test C1) and (b) protected pier with bed sill and sacrificial piles (test C9).

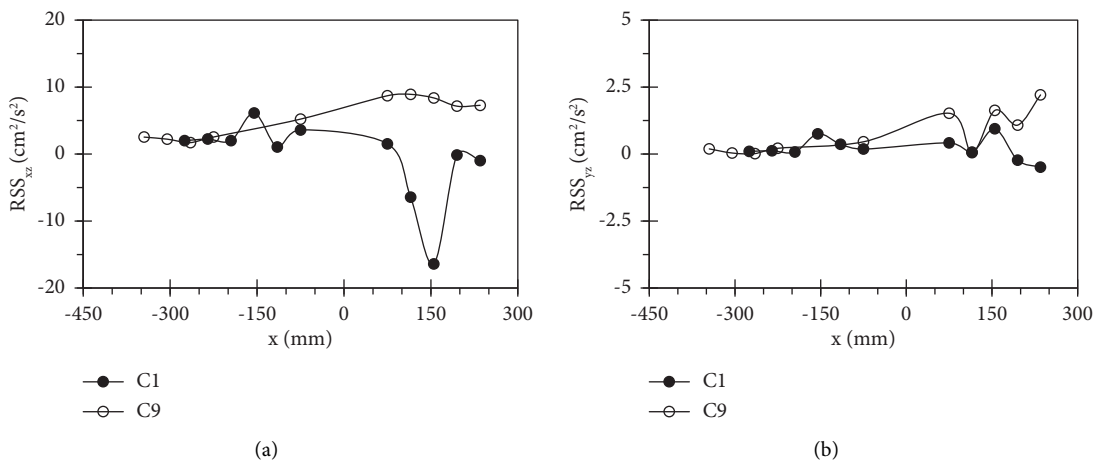

Figure 9: Longitudinal variation of Reynolds' shear stress in the channel centerline for the unprotected pier (test C1) and protected pier with bed sill and sacrificial piles (test C9): (a) RSS_{xz} and (b) RSS_{yz}.

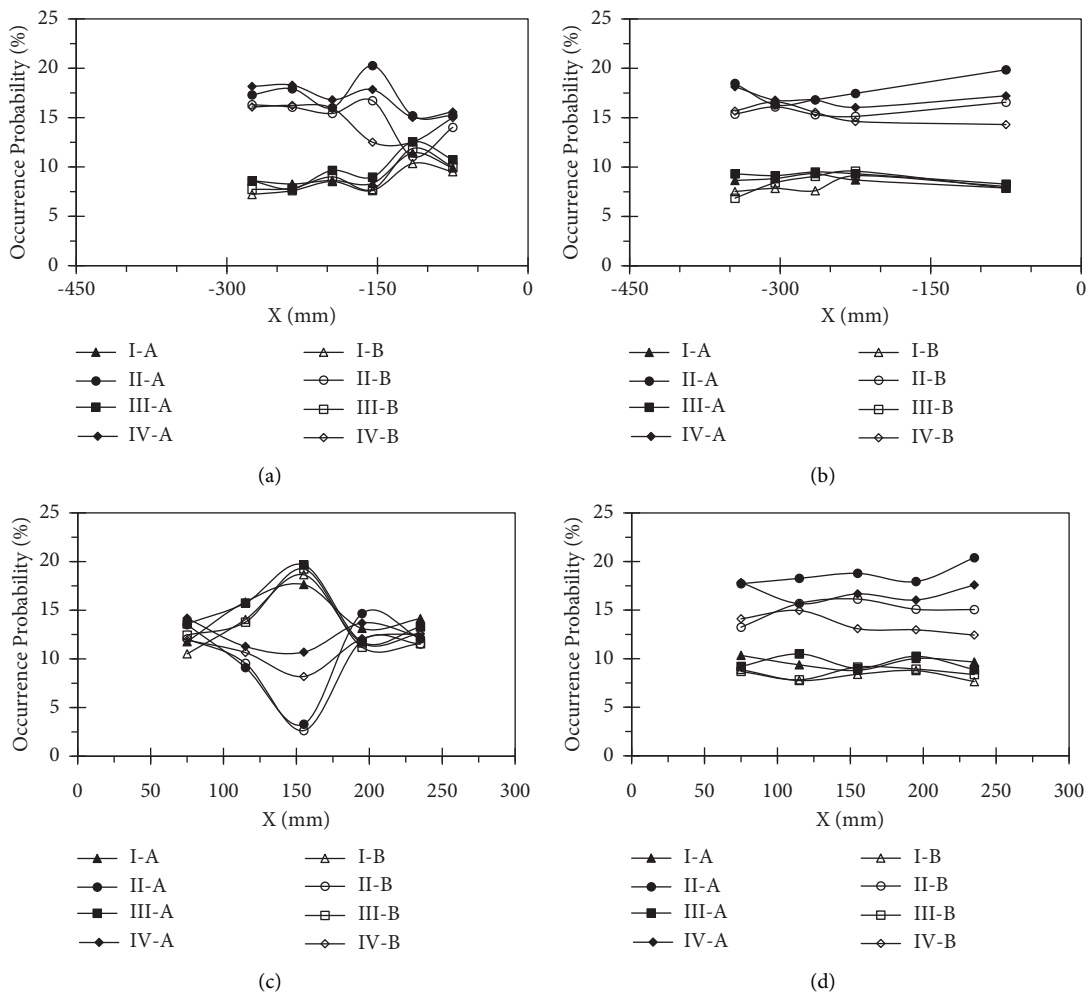

Figure 10: Longitudinal variation of the occurrence probabilities in the channel centerline for (a) upstream of C1, (b) upstream of C9, (c) downstream of C1, and (d) downstream of C9.

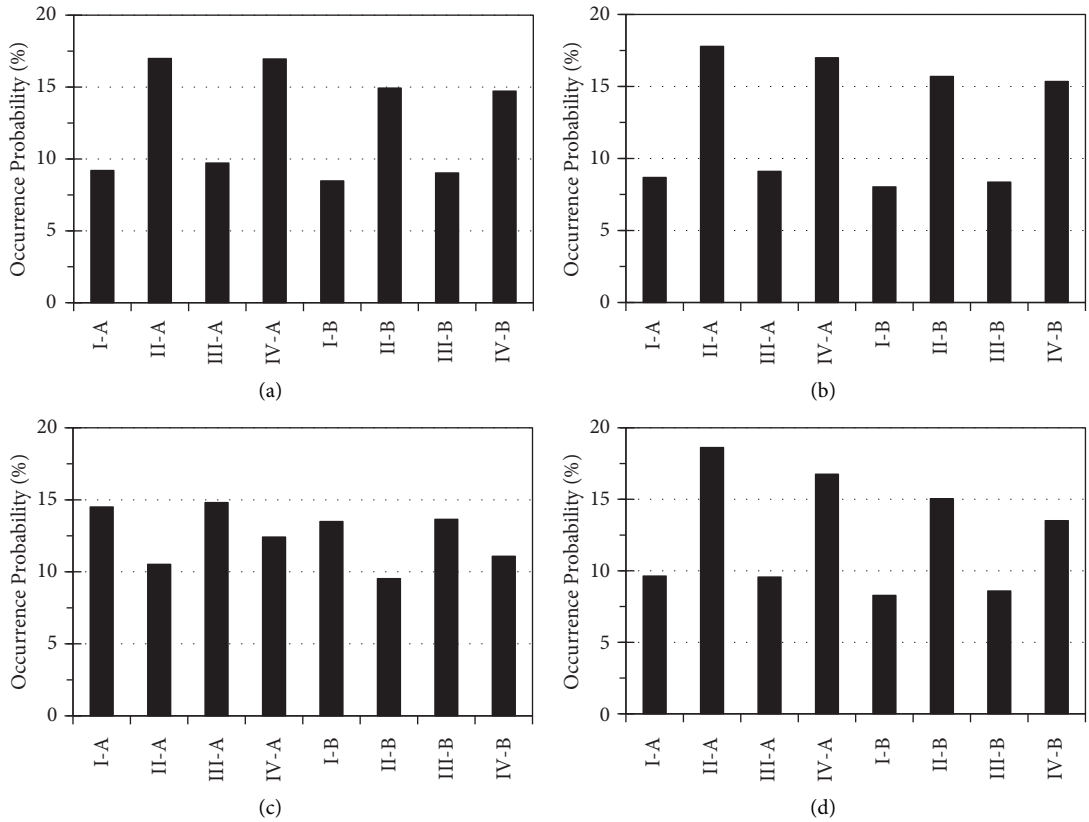

Figure 11: Average occurrence probabilities in the channel centerline for (a) upstream of C1, (b) upstream of C9, (c) downstream of C1, and (d) downstream of C9.

Table 6: Average transition probability at upstream of the unprotected pier (test C1).

	Internal				External			
	I-A ($t+1$)	II-A ($t+1$)	III-A ($t+1$)	IV-A ($t+1$)	I-B ($t+1$)	II-B ($t+1$)	III-B ($t+1$)	IV-B ($t+1$)
Internal								
I-A (t)	**46.71**	4.93	0.50	16.18	11.14	15.64	1.16	3.73
II-A (t)	3.12	**59.28**	5.65	1.89	9.94	13.35	1.99	4.77
III-A (t)	0.67	13.35	**48.83**	4.85	1.49	3.95	11.54	15.33
IV-A (t)	6.17	2.33	3.34	**57.74**	1.96	5.28	9.75	13.42
External								
I-B (t)	13.22	16.40	1.02	4.75	**45.95**	4.26	0.50	13.90
II-B (t)	11.18	14.52	1.72	5.86	2.52	**56.08**	6.46	1.66
III-B (t)	1.32	4.94	13.51	16.66	0.55	11.64	**47.12**	4.26
IV-B (t)	2.09	6.26	11.64	14.66	6.13	1.93	2.86	**54.44**

In table, among the bolded values, these values have the highest value.

Table 7: Average transition probability at upstream of the pier with bed sill and sacrificial piles (test C9).

	Internal				External			
	I-A ($t+1$)	II-A ($t+1$)	III-A ($t+1$)	IV-A ($t+1$)	I-B ($t+1$)	II-B ($t+1$)	III-B ($t+1$)	IV-B ($t+1$)
Internal								
I-A (t)	**45.40**	4.15	0.48	19.75	10.20	14.02	1.17	4.83
II-A (t)	2.80	**57.16**	6.73	2.04	8.76	15.31	2.05	5.14
III-A (t)	0.59	18.19	**44.97**	4.47	1.69	4.62	11.12	14.36
IV-A (t)	5.84	2.74	3.24	**56.44**	2.10	5.90	8.96	14.76
External								
I-B (t)	13.48	14.43	1.34	5.38	**44.61**	3.54	0.15	17.07
II-B (t)	10.42	15.28	2.03	6.69	2.28	**54.15**	7.52	1.64
III-B (t)	1.33	5.86	13.54	15.07	0.35	14.71	**45.25**	3.89
IV-B (t)	2.32	6.88	10.93	14.38	7.13	2.11	2.27	**53.96**

In table, among the bolded values, these values have the highest value.

Table 8: Average transition probability at downstream of the unprotected pier (test C1).

	Internal				External			
	I-A ($t+1$)	II-A ($t+1$)	III-A ($t+1$)	IV-A ($t+1$)	I-B ($t+1$)	II-B ($t+1$)	III-B ($t+1$)	IV-B ($t+1$)
Internal								
I-A (t)	**63.35**	2.14	1.62	9.05	8.45	10.02	3.78	1.55
II-A (t)	4.11	**54.07**	10.51	0.78	15.66	9.47	2.83	2.57
III-A (t)	1.43	7.88	**61.46**	2.21	4.61	1.57	10.28	10.54
IV-A (t)	7.38	0.87	3.26	**59.67**	1.41	2.51	16.10	8.79
External								
I-B (t)	9.36	11.10	4.08	1.96	**61.58**	1.90	1.66	8.35
II-B (t)	17.15	8.47	3.76	3.48	3.41	**51.73**	11.25	0.71
III-B (t)	4.16	2.21	11.84	12.77	1.44	7.65	**57.75**	2.18
IV-B (t)	1.86	3.58	16.10	8.96	7.30	0.74	3.19	**58.28**

In table, among the bolded values, these values have the highest value.

Table 9: Average transition probability at downstream of the pier with bed sill and sacrificial piles (test C9).

	Internal				External			
	I-A ($t+1$)	II-A ($t+1$)	III-A ($t+1$)	IV-A ($t+1$)	I-B ($t+1$)	II-B ($t+1$)	III-B ($t+1$)	IV-B ($t+1$)
Internal								
I-A (t)	**59.57**	3.22	0.37	10.73	7.61	15.49	0.93	2.08
II-A (t)	1.64	**74.18**	3.58	0.63	7.74	9.67	0.73	1.80
III-A (t)	0.48	8.45	**61.62**	3.25	1.21	1.63	9.45	13.92
IV-A (t)	4.93	0.74	2.17	**68.26**	1.24	1.89	9.59	11.15
External								
I-B (t)	10.92	15.21	1.08	2.61	**57.92**	2.37	0.42	9.48
II-B (t)	10.01	11.93	0.75	2.65	1.55	**68.94**	3.59	0.58
III-B (t)	1.34	1.66	10.85	16.95	0.37	7.59	**58.62**	2.61
IV-B (t)	1.31	2.85	10.85	13.13	5.33	0.52	1.76	**64.24**

In table, among the bolded values, these values have the highest value.

3.4. Reynolds' Shear Stress. Variations of Reynolds' shear stress near the bed for the two planes *xz* and *yz,* from upstream to downstream of the channel centerline are presented in Figure 9. Reynolds' shear stress was significantly different from upstream to downstream for both the C1 and C9 models. The results obtained for the downstream of both models, and for the position between the pier and sacrificial piles, showed a different and significant trend; however, no significant variations were found for the upstream regions in both models. Due to the high turbulence in front and behind the pier, Reynolds' stress was increased in the C9 model. The results, thus, showed that when the flow is very turbulent, the shear stress is high. A 3D analysis of bursting events was also used to investigate various flow and turbulence characteristics with higher accuracy.

3.5. Occurrence Probabilities. The contribution of occurrence probabilities related to the points near the bed for the two models C1 and C9 is shown in Figure 10. For the position in front of the pier, the highest occurrence probability for unprotected and protected piers is related to events IV-A and II-A, respectively. Therefore, the use of BSSP caused sediments to be suspended and inclined to move to the upper edge of the scour hole, until they would move towards the downstream side of the pier; as a result, the scour depth could be decreased. The results obtained for the upstream of the pier showed that the sweep and ejection events had increased while approaching the pier.

According to Figure 10(d), events II-A, IV-A, II-B, and IV-B have the highest occurrence probability and events I-A, III-A, I-B, and III-B have the lowest occurrence probability. The increase in ejection and sweep events in two classes A and B downstream of the pier could be mostly due to the formation of two symmetrical scour holes downstream of the bed sill. According to the obtained results, although the occurrence probabilities of events causing sediment transport increased in the region between the pier and sacrificial piles, as well as downstream of the pier, eventually, the simultaneous combination of BSSP effectively reduced the scour depth in front of the pier. This is because the sediments scoured from around the sacrificial piles were deposited on inside the scour hole in front of the pier. On the other hand, the bed sill, by reducing the strength of wake vortices behind the pier, could reduce the transport of sediment from the front of the pier to the back of the pier. As a result, the scour depth could be reduced by using a simultaneous combination of BSSP.

Figure 11 shows the occurrence probabilities' contribution in classes A and B. The highest average occurrence probabilities in the upstream of both models were related to event II-A. In the downstream of the pier, the highest average occurrence probabilities for the C1 and C9 models were related to III-A and II-A events, respectively. Ejection events produced pulses with a low speed from the boundary layer into the main flow towards the water surface and against the flow direction. Inward interaction events could

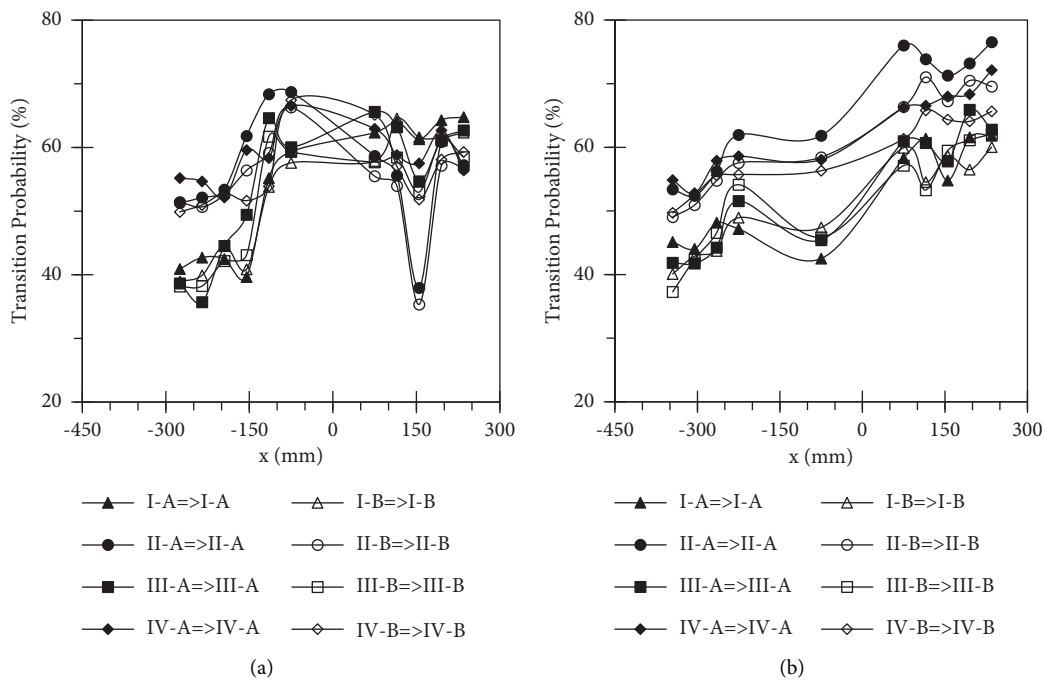

Figure 12: Longitudinal variations of the stable transition probabilities in the channel centerline for (a) unprotected pier (test C1) and (b) protected pier with bed sill and sacrificial piles (test C9).

produce pulses with a low speed from the main flow into the boundary layer towards the bed surface and against the flow direction [31].

3.6. Transition Probabilities. Based on the sign of the velocity fluctuations at a moment of time, one of the events of the bursting process could occur. Transition probabilities in octant analysis are classified into 64 sections; each of these sections shows the probability of movement from one state to another. By using the Markov process, the transition probabilities in these 64 sections were determined for points near the bed in the centerline of the C1 and C9 models. For the upstream and downstream of these two models, the average transition probabilities were determined separately. The results of the average transition probabilities are presented in Tables 6–9 for the upstream and downstream of the C1 and C9 models, respectively. According to the 64 probable movements, three specific movements (marginal movement, cross-movement, and stable movement) were recognizable [31, 34, 59]. Marginal movements such as II-B $\longleftrightarrow$ III-B, cross-movements such as II-B $\longleftrightarrow$ IV-B, and stable movements such as II-B $\longleftrightarrow$ II-B could be observed.

Stable movement occurs when each of the eight octant zone events at time (t) stays in the same zone after a one-time step ($t+1$). This type of movement has the highest transition probability (Tables 6–9). Therefore, this section focuses on the transition probabilities of stable movement. These results are consistent with those of the previous studies [25, 31, 60]. The highest transition probability in the upstream of both C1 and C9 models was related to stable movement II-A $\longleftrightarrow$ II-A (Tables 6 and 7); meanwhile, in the downstream of the pier, the highest transition probability for the C1 model was related to I-A $\longleftrightarrow$ I-A (Table 8); for the C9 model, it was related to II-A $\longleftrightarrow$ II-A (Table 9). These values are bolded. The transition probabilities of stable movement in the upstream of the pier for the C9 model were decreased as compared to the C1 model; meanwhile, in the downstream of the pier, except for I-A $\longleftrightarrow$ I-A and I-B $\longleftrightarrow$ I-B movements, the transition probabilities of stable movement for the C9 model were increased, as compared to the C1 model. Examination of the results showed that the events with the highest occurrence probability also had the highest stable transition probability. It could also be stated that the occurrence probabilities alone may not be able to determine the situation of bursting events. Therefore, the results of the transition probabilities could be regarded as a complement to the results of occurrence probabilities, but in this study, it does not help much to investigate the sediment condition and their type of movement. In addition, as can be seen in Figure 12, the longitudinal variations of the stable transition probabilities from the upstream to the downstream of both pier models could be seen.

4. Conclusions

This study investigated the combination of two countermeasures (BSSP) in terms of efficiency. It was found that this combination was quite effective in reducing scour depth. The best configurations of BSSP showed an efficiency of 51.1% in reducing the local scour depth. The combination of BSSP could be, therefore, recommended as a suitable solution in design and construction to reduce the local scour.

In order to investigate the complex flow structure and how it could affect the scour mechanism, the coherent flow structure was carried out at the points near the bed from the upstream to the downstream of the C1 and C9 models. A 3D analysis of the bursting process was used to identify the most probable bursting events. It was found that the stable transition probabilities, among other movements, had the highest transition probabilities. Also, the results showed that the event that had the highest occurrence probability also had the highest transition probability. The effect of the simultaneous use of BSSP on the reduction of the scour depth was confirmed by the results obtained from the investigation of the flow structure [61].

Notations

B: Channel width
D: Circular pier diameter
D_p: Sacrificial pile diameter
d_{16}: Size below which 16% of all particles are finer
d_{50}: Mean size of sediment particle
d_{84}: Size below which 84% of all particles are finer
ds: Local scour depth
d_{se}: Scour depth at the end of the test for protected pier
d_{se0}: Scour depth at the end of the test for unprotected pier
f: Unknown function
Fr: Froude number
Fr_P: Pier Froude number $(U/\sqrt{gD})$
g: Acceleration of gravity
L_{bs}: Distance between the bed sill and pier
N_p: Number of piles
N: Number of instantaneous velocity samples
N_t: Total number of events
n_i: Number of events in time series in zone i
$n_{i\longrightarrow j}$: Number of transition events
n_k: Number of events in each zone
P_k: Occurrence probability
$P_{i\longrightarrow j}$: Transition probability
Q: Flow discharge
S_p: Distance between the piles
t: Time
U: Mean approach flow velocity
U_{*c}: Critical shear velocity
U_c: Critical flow velocity
u_i: Instantaneous velocity in the streamwise direction
u': Velocity fluctuation in the streamwise direction
$\overline{u}$: Temporal average velocity in the streamwise direction
v_i: Instantaneous velocity in the vertical direction
v': Velocity fluctuation in the vertical direction
$\overline{v}$: Temporal average velocity in the vertical direction
w_i: Instantaneous velocity in the transverse direction
w': Velocity fluctuation in the transverse direction
$\overline{w}$: Temporal average velocity in the transverse direction
X: Displacement distance
y: Flow depth
α: Angle of the wedge
β: Deviation angle between the approach flow and pier axis (skew angle)
ρ: Water density
ρ_s': Submerged sediment density
ν: Kinematic viscosity of water
σ_g: Geometric standard deviation $(\sqrt{(d_{84}/d_{16})})$.

Data Availability

The data generated or analyzed during this study are available from the corresponding author upon reasonable request.

Disclosure

An earlier version of this article is available as a preprint at the following link: https://assets.researchsquare.com/files/rs-2416854/v1_covered.pdf?c=1672662498.

Conflicts of Interest

The authors declare that they have no conflicts of interest.

References

[1] S. Dey, S. K. Bose, and G. L. Sastry, "Clear water scour at circular piers: a model," *Journal of Hydraulic Engineering*, vol. 121, no. 12, pp. 869–876, 1995.
[2] X. Kong and C. S. Cai, "Scour effect on bridge and vehicle responses under bridge-vehicle-wave interaction," *Journal of Bridge Engineering*, vol. 21, no. 4, Article ID 04015083, 2016.
[3] S. Khaple, P. R. Hanmaiahgari, R. Gaudio, and S. Dey, "Splitter plate as a flow-altering pier scour countermeasure," *Acta Geophysica*, vol. 65, no. 5, pp. 957–975, 2017.
[4] S. Li, S. He, H. Li, and Y. Jin, "Scour depth determination of bridge piers based on time-varying modal parameters: application to hangzhou bay bridge," *Journal of Bridge Engineering*, vol. 22, no. 12, Article ID 04017107, 2017.
[5] E. Sanadgol, M. Heidarpour, and R. Mohammadpour, "Reduction of local scouring at round-nosed rectangular piers using a downstream bed sill," *Journal of the South African Institution of Civil Engineers*, vol. 63, no. 3, pp. 1–9, 2021.
[6] B. W. Melville and A. C. Hadfield, "Use of sacrificial piles as pier scour countermeasures," *Journal of Hydraulic Engineering*, vol. 125, no. 11, pp. 1221–1224, 1999.
[7] E. Izadinia and M. Heidarpour, "Simultaneous use of cable and collar to prevent local scouring around bridge pier," *International Journal of Sediment Research*, vol. 27, no. 3, pp. 394–401, 2012.
[8] A. Tafarojnoruz, R. Gaudio, and F. Calomino, "Evaluation of flow-altering countermeasures against bridge pier scour," *Journal of Hydraulic Engineering*, vol. 138, no. 3, pp. 297–305, 2012a.
[9] N. B. Singh, T. T. Devi, and B. Kumar, "The local scour around bridge piers-a review of remedial techniques," *ISH Journal of Hydraulic Engineering*, vol. 28, no. sup1, pp. 527–540, 2022.
[10] C. Grimaldi, R. Gaudio, F. Calomino, and A. H. Cardoso, "Control of scour at bridge piers by a downstream bed sill," *Journal of Hydraulic Engineering*, vol. 135, no. 1, pp. 13–21, 2009a.
[11] M. A. Haque, M. M. Rahman, G. M. T. Islam, and M. A. Hussain, "Scour mitigation at bridge piers using

sacrificial piles," *International Journal of Sediment Research*, vol. 22, no. 1, pp. 49–59, 2007.

[12] C. Grimaldi, R. Gaudio, F. Calomino, and A. H. Cardoso, "Countermeasures against local scouring at bridge piers: slot and combined system of slot and bed sill," *Journal of Hydraulic Engineering*, vol. 135, no. 5, pp. 425–431, 2009b.

[13] R. Gaudio, A. Tafarojnoruz, and F. Calomino, "Combined flow-altering countermeasures against bridge pier scour," *Journal of Hydraulic Research*, vol. 50, no. 1, pp. 35–43, 2012.

[14] Y. M. Chiew, "Scour protection at bridge piers," *Journal of Hydraulic Engineering*, vol. 118, no. 9, pp. 1260–1269, 1992.

[15] S. Soltani-Gerdefaramarzi, H. Afzalimehr, Y. M. Chiew, and J. Gallichand, "Reduction of pier scour using bed suction and jet injection," *Proceedings of the Institution of Civil Engineers Water Management*, vol. 167, no. 2, pp. 105–114, 2014.

[16] A. T. Moncada-M, J. Aguirre-Pe, J. C. Bolivar, and E. J. Flores, "Scour protection of circular bridge piers with collars and slots," *Journal of Hydraulic Research*, vol. 47, no. 1, pp. 119–126, 2009.

[17] M. B. Mashahir, A. R. Zarrati, M. J. Rezaei, and M. Zokaei, "Effect of collar and bars in reducing the local scour around cylindrical bridge piers," *International Journal of Engineering*, vol. 22, no. 4, pp. 333–342, 2009.

[18] N. Shahkarami, "Evaluation the performance of bed sill, collar and their combination in scour protection of cylindrical bridge pier," *Journal of Civil & Environmental Engineering*, vol. 47, no. 4, pp. 113–121, 2018.

[19] M. Mazloom, S. R. Khodashenas, and K. Esmaili, "Evaluation of effect of the submerged vanes and slot on reduction of local scour around bridge," *Iranian Journal of Irrigation and Drainage*, vol. 12, no. 5, pp. 1097–1106, 2018.

[20] S. Zomorodian, H. Ghafari, and Z. Ghasemi, "Separated and combined effects of sacrificial piles, collar and slot on reduction of the local scour around the bridge piers," *Journal of Hydraulics*, vol. 11, no. 2, pp. 77–85, 2016.

[21] M. Aghli and S. Zomorodian, "Effect of cable and collar on scouring depth around cylindrical bridge pier in meandering river," *Journal of Irrigation Sciences and Engineering*, vol. 36, no. 3, pp. 31–40, 2013.

[22] P. Shojaei, D. Farsadizadeh, and A. Hoseinzadeh Dalir, "Effects of combined submerged vanes and collar on the scour reduction around cylindrical bridge piers," *Journal of Water and Soil Science*, vol. 15, no. 57, pp. 23–33, 2011.

[23] A. Tafarojnoruz, R. Gaudio, and F. Calomino, "Bridge pier scour mitigation under steady and unsteady flow conditions," *Acta Geophysica*, vol. 60, no. 4, pp. 1076–1097, 2012b.

[24] V. J. Vahdati, S. Yaghoubi, A. Torabipour, J. A. Correia, T. Fazeres-Ferradosa, and F. Taveira-Pinto, "Combined solutions to reduce scour around complex foundations: an experimental study," *Marine Systems and Ocean Technology*, vol. 15, no. 1, pp. 81–93, 2020.

[25] E. Gerami, M. Heidarpour, and R. M. Ghalati, "Effect of simultaneous use of cable and bed sill scour countermeasures around a cylindrical pier," *Proceedings of the Institution of Civil Engineers Water Management*, vol. 176, no. 6, pp. 277–290, 2023.

[26] Y. M. Chiew and B. W. Melville, "Local scour around bridge piers," *Journal of Hydraulic Research*, vol. 25, no. 1, pp. 15–26, 1987.

[27] A. Tafarojnoruz, R. Gaudio, C. Grimaldi, and F. Calomino, "Required conditions to achieve the maximum local scour depth at a circular pier," in *Proceedings of the XXXII Convegno Nazionale di Idraulica e Costruzioni Idrauliche. Farina*, Springer, Palermo, Italy, 2010b.

[28] A. Tafarojnoruz, R. Gaudio, and S. Dey, "Flow-altering countermeasures against scour at bridge piers: a review," *Journal of Hydraulic Research*, vol. 48, no. 4, pp. 441–452, 2010a.

[29] E. Izadinia, M. Heidarpour, and A. J. Schleiss, "Investigation of turbulence flow and sediment entrainment around a bridge pier," *Stochastic Environmental Research and Risk Assessment*, vol. 27, no. 6, pp. 1303–1314, 2013.

[30] A. Keshavarzi, C. K. Shrestha, M. R. Zahedani, J. Ball, and H. Khabbaz, "Experimental study of flow structure around two in-line bridge piers," *Proceedings of the Institution of Civil Engineers Water Management*, vol. 171, no. 6, pp. 311–327, 2018.

[31] A. Keshavarzi, B. Melville, and J. Ball, "Three-dimensional analysis of coherent turbulent flow structure around a single circular bridge pier," *Environmental Fluid Mechanics*, vol. 14, no. 4, pp. 821–847, 2014.

[32] S. J. Mianaei and A. Keshavarzi, "Study of near bed stochastic turbulence and sediment entrainment over the ripples at the bed of open channel using image processing technique," *Stochastic Environmental Research and Risk Assessment*, vol. 24, no. 5, pp. 591–598, 2010.

[33] F. S. Esfahani and A. Keshavarzi, "Effect of different meander curvatures on spatial variation of coherent turbulent flow structure inside ingoing multi-bend river meanders," *Stochastic Environmental Research and Risk Assessment*, vol. 25, no. 7, pp. 913–928, 2011.

[34] F. S. Esfahani and A. Keshavarzi, "Dynamic mechanism of turbulent flow in meandering channels: considerations for deflection angle," *Stochastic Environmental Research and Risk Assessment*, vol. 27, no. 5, pp. 1093–1114, 2013.

[35] R. Ettema, *Scour at Bridge Piers. Report No. 216. School of Engineering*, University of Auckland, Auckland, New Zealand, 1980.

[36] E. M. Laursen and A. Toch, *Scour Around Bridge Piers and Abutments*, Iowa Highway Research Board, Ames, IA, USA, 1956.

[37] A. J. Raudkivi, *Loose Boundary Hydraulics*, Pergamon, Oxford, UK, 1990.

[38] M. F. Mia and H. Nago, "Design method of time-dependent local scour at circular bridge pier," *Journal of Hydraulic Engineering*, vol. 129, no. 6, pp. 420–427, 2003.

[39] A. H. Cardoso and R. Bettess, "Effects of time and channel geometry on scour at bridge abutments," *Journal of Hydraulic Engineering*, vol. 125, no. 4, pp. 388–399, 1999.

[40] V. Kumar, K. G. R. Raju, and N. Vittal, "Reduction of local scour around bridge piers using slots and collars," *Journal of Hydraulic Engineering*, vol. 125, no. 12, pp. 1302–1305, 1999.

[41] B. W. Melville and Y. M. Chiew, "Time scale for local scour at bridge piers," *Journal of Hydraulic Engineering*, vol. 125, no. 1, pp. 59–65, 1999.

[42] S. Franzetti, S. Malavasi, and C. Piccinin, "Sull'erosione alla base delle pile di ponte in acque chiare" [On the erosion at the base of bridge piers in clear water]," *Proceedings of the XXIV Convegno di Idraulica e Costruzioni Idrauliche. GNDCI-CNR*, pp. 13–24, Springer, Perugia, Italy, 1994.

[43] N. Vittal, U. C. Kothyari, and M. Haghighat, "Clear-water scour around bridge pier group," *Journal of Hydraulic Engineering*, vol. 120, no. 11, pp. 1309–1318, 1994.

[44] A. Masjedi, M. Shafaei-Bejestan, and A. Esfandi, "Experimental study on local scour around single oblong pier fitted with a collar in a 180 degree flume bend," *International Journal of Sediment Research*, vol. 25, no. 3, pp. 304–312, 2010.

[45] D. G. Goring and V. I. Nikora, "Despiking acoustic Doppler velocimeter data," *Journal of Hydraulic Engineering*, vol. 128, no. 1, pp. 117–126, 2002.
[46] L. Ge, S. O. Lee, F. Sotiropoulos, and T. Sturm, "3D unsteady RANS modeling of complex hydraulic engineering flows. II: model validation and flow physics," *Journal of Hydraulic Engineering*, vol. 131, no. 9, pp. 809–820, 2005.
[47] A. A. Beheshti and B. Ataie-Ashtiani, "Experimental study of three-dimensional flow field around a complex bridge pier," *Journal of Engineering Mechanics*, vol. 136, no. 2, pp. 143–154, 2010.
[48] S. Dey, D. Swargiary, S. Sarkar, H. Fang, and R. Gaudio, "Self-similarity in turbulent wall-wake flow downstream of a wall-mounted vertical cylinder," *Journal of Hydraulic Engineering*, vol. 144, no. 6, Article ID 04018023, 2018.
[49] G. Oliveto and W. H. Hager, "Temporal evolution of clear-water pier and abutment scour," *Journal of Hydraulic Engineering*, vol. 128, no. 9, pp. 811–820, 2002.
[50] B. B. Barkdoll, B. W. Melville, and Y. M. Chiew, "Time scale for local scour at bridge piers," *Journal of Hydraulic Engineering*, vol. 126, no. 10, pp. 793–795, 2000.
[51] J. Guo, "Semi-analytical model for temporal clear water scour at prototype piers," *Journal of Hydraulic Research*, vol. 52, no. 3, pp. 366–374, 2014.
[52] B. W. Melville and D. M. Dongol, "Bridge pier scour with debris accumulation," *Journal of Hydraulic Engineering*, vol. 118, no. 9, pp. 1306–1310, 1992.
[53] H. Hamidifar, D. Mohammad Ali Nezhadian, and I. Carnacina, "Experimental study of debris-induced scour around a slotted bridge pier," *Acta Geophysica*, vol. 70, no. 5, pp. 2325–2339, 2022a.
[54] H. Hamidifar, S. M. B. Shahabi-Haghighi, and Y. M. Chiew, "Collar performance in bridge pier scour with debris accumulation," *International Journal of Sediment Research*, vol. 37, no. 3, pp. 328–334, 2022b.
[55] W. Zhang, I. Nistor, and C. D. Rennie, "Temporal evolution of the hydrodynamic loading due to dynamic debris jam on bridge pier," *Journal of Fluids and Structures*, vol. 123, Article ID 103997, 2023.
[56] H. Hamidifar, M. H. Omid, and M. Nasrabadi, "Reduction of scour using a combination of riprap and bed sill," *Proceedings of the Institution of Civil Engineers Water Management*, vol. 171, no. 5, pp. 264–270, 2018a.
[57] H. Hamidifar, M. Nasrabadi, and M. H. Omid, "Using a bed sill as a scour countermeasure downstream of an apron," *Ain Shams Engineering Journal*, vol. 9, no. 4, pp. 1663–1669, 2018b.
[58] D. Mohammad Ali Nezhadian and H. Hamidifar, "Effects of floating debris on flow characteristics around slotted bridge piers: a numerical simulation," *Water*, vol. 16, no. 1, p. 90, 2023.
[59] V. J. Vahdati, A. Ahmadi, A. Abedini, and M. Heidarpour, "Evaluation of the simultaneous combination of bed sill and sacrificial piles in the reduction of local scour depth around the bridge pier and three-dimensional analysis of turbulent flow structure around them," *Research Square*, vol. 2023, 2023.
[60] A. Keshavarzi and A. Gheisi, "Stochastic nature of three-dimensional bursting events and sediment entrainment in vortex chamber," *Stochastic Environmental Research and Risk Assessment*, vol. 21, no. 1, pp. 75–87, 2006.
[61] S. J. Kline, W. C. Reynolds, F. A. Schraub, and P. W. Runstadler, "The structure of turbulent boundary layers," *Journal of Fluid Mechanics*, vol. 30, no. 4, pp. 741–773, 1967.